Refractivities of H_2, He, O_2, CO, and Kr for $168 \leq \lambda \leq 288$ nm

Peter L. Smith
Center for Astrophysics, Harvard College Observatory and Smithsonian Astrophysical Observatory, Cambridge, Massachusetts 02138

Martin C. E. Huber
Atomic Physics and Astrophysics Group, Federal Institute of Technology (ETH-Z), CH-8006 Zürich, Switzerland and Center for Astrophysics, Harvard College Observatory and Smithsonian Astrophysical Observatory, Cambridge, Massachusetts 02138

W. H. Parkinson
Center for Astrophysics, Harvard College Observatory and Smithsonian Astrophysical Observatory, Cambridge, Massachusetts 02138
(Received 18 November 1975)

Precision measurements of the refractivities of H_2, He, O_2, CO, and Kr were made in the wavelength range 168–288 nm. By using a 1.2-m-long test cell and by keeping the test gas at accurately determined conditions near atmospheric pressure and room temperature, we were able to achieve accuracies (90% confidence limit) for the absolute refractivities that ranged from ±0.1% to ±1.0% depending upon the gas and wavelength range. For a given gas, the ratio of refractivities at any two wavelengths has a smaller uncertainty. For H_2, CO, and O_2, our results are for wavelengths shorter than those of previous measurements and, for He and Kr, our uncertainties are less than those of other measurements. For He our refractivities agree with the theoretical ones, but in the case of H_2 our results are about 1% larger than the theoretical values. At the upper end of the wavelength range studied, our data are in agreement with previous measurements on H_2, CO, and Kr. For O_2 our results indicate that the hitherto available data are too large by amounts ranging from 0.8% to 10%.

I. INTRODUCTION

The indices of refraction of atomic and molecular gases reflect the properties of the constituents of the gases. For example, the refractive index $n(\lambda)$ is related to the dielectric polarizability $\alpha_d(\lambda)$ and to the absorption oscillator strengths f_i for transitions of wavelengths λ_i by the expression

$$\frac{n^2-1}{n^2+2}=\frac{4}{3}\pi N\alpha_d=\frac{\alpha^2 N a_0 \lambda^2}{3\pi}\sum_i \frac{\lambda_i^2 f_i}{\lambda^2-\lambda_i^2}, \tag{1}$$

where α is the fine-structure constant, N is the number density of atoms or molecules, and a_0 is the Bohr radius.[1,2] The summation S is taken over discrete as well as continuous transitions of the atoms or molecules concerned. In the limit $n \simeq 1$, Eq. (1) becomes

$$n-1 \equiv R \simeq 2\pi N\alpha_d=\frac{\alpha^2 N a_0 \lambda^2}{2\pi}\sum_i \frac{\lambda_i^2 f_i}{\lambda^2-\lambda_i^2}, \tag{1a}$$

where R is the refractivity.

In addition, the refractive index is related to the Rayleigh-scattering cross section,[1-4] which under certain simplifying assumptions[3] can be expressed as

$$Q=(128\pi^5/9\lambda^4)[3\alpha_d^2(\lambda)+\tfrac{2}{3}\gamma_d^2(\lambda)], \tag{2}$$

where $\gamma_d(\lambda)$ is the dipole polarizability anisotropy. Rayleigh-scattering cross sections are of considerable astrophysical interest for the interpretation of the spectra of the giant planets[4,5] and for the determination of the opacity of the atmospheres of late-type, hydrogen-deficient giant and supergiant stars.[6]

A review of the literature shows that the most comprehensive listing of refractivity data is given in *International Critical Tables*.[7] For most gases, these data are limited to wavelengths longer than 230 nm. Leonard[1] gives a critical compilation of data for the rare gases.

The most accurate refractivity determinations have been made using interferometric techniques. Peck and co-workers have reported accurate measurements for $\lambda \gtrsim 500$ nm for Ar,[8] N_2,[9] He,[10] and air.[11] Pery-Thorne[12] extended such measurements to the vacuum ultraviolet and gave the refractivity of Ar at 160 nm. Abjean and co-workers have determined refractivities for N_2 and Ar,[13] He and Ne,[14] Xe and Kr,[15] and CO_2 (Ref. 16) at wavelengths between 180 and 260 nm. Recently, Smith *et al.*[17] published refractivity data for Kr from 168 to 288 nm, and Bideau-Méhu *et al.*[18] reported refractivity measurements for Ne, Ar, and N_2 at 164.1 nm, for He, Ne, Xe, Ar, and N_2 at 170.2 nm, and for Kr from 164 to 229 nm.

Huber and Tondello[19] and Chaschina and co-workers[20,21] have used the spectral line-shift method of Wilkinson[22] to study He, Xe and Kr, and Ar, respectively, in the vacuum-ultraviolet wavelength region. In addition, Heddle and colleagues[23-25] have published refractivities at the Lyman-α line (121.6 nm) and at longer vacuum-ultraviolet wavelengths. These data for H_2, N_2, Ar, Kr, and Xe

are derived from Rayleigh-scattering and Cherenkov-radiation measurements. Some early data are summarized by Zaidel' and Shreider.[26]

Most of the data for $\lambda \leq 200$ nm are of low precision or are not in agreement with longer-wavelength measurements. For example, the data of Huber and Tondello[19] and of Abjean *et al.*[14] on He have an experimental uncertainty of $\pm 2\%$; this is in excess of the estimated uncertainties in current theoretical calculations for a two-electron system by Victor *et al.*[27] and Victor.[28] The data of Chaschina and Shreider[20] for Kr are given after smoothing by a three-term Sellmeir formula and the accuracy is difficult to determine. The data of Abjean *et al.*[15] for Kr have been shown to be too large by about 4%.[17,18] For H_2, the theoretical calculations of Ford[29] are about 1% lower than the existing experimental data.[30,31]

The results of our measurements for He and Kr are more accurate than other experimentally determined refractivities. For H_2, CO, and O_2 our values are for wavelengths shorter than those of previous laboratory studies. In particular, we report the first precise measurements of the refractive index of H_2 between 168 and 185 nm, of CO between 168 and 238 nm, and of O_2 between 184 and 275 nm.

II. EXPERIMENTAL METHOD AND UNCERTAINTIES

A. Equipment and method

Our refractivity measurements were made with a Mach-Zehnder interferometer *in vacuo*. This instrument and associated equipment (i.e., light source and spectrograph/spectrometer) have been described in detail by Banfield *et al.*[32] and are shown schematically in Fig. 1. The interferometer optics are made of fused silica and, consequently, the smallest wavelength at which measurements were possible was 167 nm. The main vacuum chamber as well as the compensation chamber of the interferometer (see Fig. 1) were evacuated to a pressure of less than 5×10^{-7} Torr during the measurements.

When an absorption cell of length l is filled to pressure P (given in Torr) with an ideal gas of refractive index $n(\lambda)$ and temperature T (given in K), then the fringe order observed at wavelength λ is

$$N = \frac{[n(\lambda) - 1]l}{\lambda} \frac{P}{760} \frac{273.15}{T} + N_0, \tag{3}$$

where N_0 is the fringe order observed at $P = 0$.

Our refractivity measurements were made using both photographic and photoelectric methods. The procedure comprised four major steps.

First, the fringes were aligned parallel to the entrance slit and the spectrometer was set at a given wavelength. The pressure was slowly increased from zero to slightly (about 5 Torr) above ambient pressure, while fringes, corresponding to changes in the optical path length, were detected photoelectrically. In order to count the fringes, the sinusoidal output of the photomultiplier was recorded on a strip chart. In addition, the output was converted to a pulsed signal which was counted with a digital counter.

Second, the pressure was held constant at

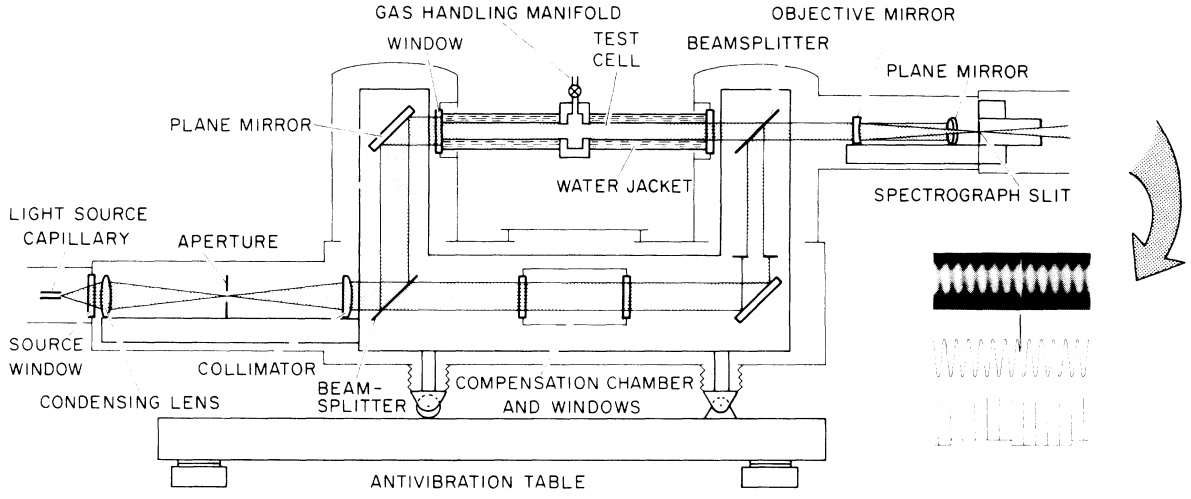

FIG. 1. Schematic of apparatus for refractivity measurements. During a measurement, the spectral display of fringes in the focal plane of the spectrograph can be recorded photoelectrically as well as by photograph, as indicated in the inset. The inset also shows an emission line superimposed on the fringe pattern.

$P \simeq 1$ atm + 5 Torr while the wavelength was scanned. The fringes were again detected and counted photoelectrically. Because of imperfections in the interferometer beam splitters, the fringe contrast decreased as we scanned to shorter wavelengths. Below about 200 nm the signal-to-noise ratio had decreased to the point where the photoelectric counting system became unreliable.

Consequently, the third step in our measurement procedure was to photograph the fringe pattern at the wavelengths between 165 and 250 nm. Emission lines, which appeared superimposed on the continuum from our light source, served as wavelength standards. This enabled us to register the fringe count from the chart recordings with that of the photographs. A photograph of fringes and a schematic diagram of the equivalent photoelectric signals are shown as part of Fig. 1.

The fourth and final major step in the measurement procedure was the evacuation of the absorption cell, while the wavelength was held constant. The fringes were again counted photoelectrically.

The experimental procedure can be summarized with the help of Fig. 2, which shows the relationship between P, λ, and N for a typical measurement. Most data are the average of two or more measurements using this procedure.

B. Corrections and reduction to standard conditions

After the above procedure was completed, two corrections had to be made to the fringe-count data.

First, because the thicknesses of the beam splitters and windows in the two interferometer beams were not equal, there was a residual layer of fused silica in the reference beam. The refractive index of this residual layer was dependent upon wavelength, and consequently spurious fringes, which we called "quartz" fringes, were included in the measured fringe count as the wavelength was scanned. The quartz fringes were measured before and after each refractivity measurement by scanning wavelength when the absorption cell was evacuated. The quartz-fringe correction was not large and could be accurately determined. For example, about four quartz fringes were observed when the wavelength was scanned from 288 to 222 nm and about 18 quartz fringes occurred between 222 and 168 nm. In Fig. 2, the effect on the photoelectric scans of the presence of a residual layer of fused silica in the reference beam is shown. The quartz fringes, introduced in part II of the cycle, will bring part IV of the cycle to negative N at zero pressure. By closing the cycle with part V we recorded the quartz fringes and at the end point of the cycle ($\lambda = 288$ nm, $P = 0$) the net fringe count should be zero.

The second correction was required because the net fringe count was usually not zero. This can be explained by a fringe drift which is thought to be caused by temperature changes of the interferometer structure and/or backlash in interferometer-component adjustment mechanisms. The total measured drift observed at the cycle endpoint was usually about 3 fringes. Repeated monitoring of the drift over an extended period indicated that the drift was approximately constant. Typical corrections to the fringe counts ranged from 2 ± 0.5 for $\lambda = 288$ nm to 3 ± 0.5 for $\lambda = 220$ nm.

The reduction of measured refractivities to standard conditions ($T_0 = 273.15$ K, $P_0 = 760$ Torr is discussed by Mansfield and Peck.[10] They give

$$\frac{n_0 - 1}{n - 1} = \frac{P_0 T}{P T_0} \left\{ \frac{Z}{Z_0} \left[1 + \frac{n_0 - 1}{6} \left(1 - \frac{P T_0}{P_0 T} \right) \right] \right\} . \qquad (4)$$

For the conversion of our data to standard conditions we used values of compressibility Z given by Hilsenrath[33] or virial coefficients given by Sengers, Klein, and Gallagher.[34] Because all of our absolute-refractivity measurements were made with P and T near standard conditions, the value of the term within the braces in Eq. (4) deviated from unity by a fractional amount that was about an order of magnitude smaller than our fractional experimental uncertainties.

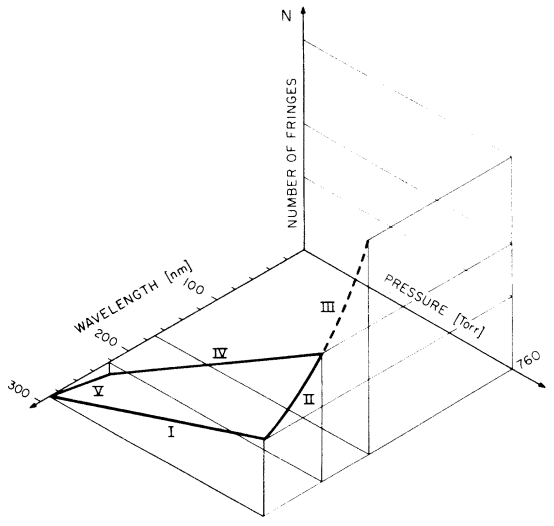

FIG. 2. Schematic representation of measurement procedure. Labeled sections of heavy line correspond to (I), filling of test gas at fixed wavelength; (II), wavelength scanning at fixed pressure; (III), fringe pattern at short wavelength being photographed; (IV), evacuation of test cell at fixed wavelength; (V), returning to initial wavelength with zero pressure, i.e., scanning quartz fringes. In this figure we have assumed that N_0 of Eq. (3) was zero.

C. Special procedures

It was occasionally necessary to deviate from the techniques outlined in Sec. II A. In some cases (to be discussed in this section) we had to use pressures smaller than 760 Torr. This resulted in fewer fringes and, correspondingly, in larger uncertainties in the fringe counts than were usually obtained.

In the case of Kr, we made one photographic measurement from 244 to 168 nm at a pressure of 0.2 atm. In this way we reduced the number of fringes on the plate and thus facilitated their counting at short wavelengths. The resulting data were then normalized by making them agree with the data measured in the normal manner for wavelengths between 197 and 244 nm. This procedure resulted in a higher accuracy than would have been possible for one which would have had to rely on pressure measurements of a fractional atmosphere with our apparatus.

With CO it was impossible to obtain fringes below 220 nm with $P \simeq 1$ atm because of absorption by the bands of the fourth positive system. Photographic measurements were, however, possible with $P \simeq 100$ Torr. The results obtained at a fraction of atmospheric pressure were put onto the absolute scale in the way described above for the case of Kr.

This procedure could not be used to study refractivities of O_2 at wavelengths affected by absorption by the Schumann-Runge system ($\lambda < 197$ nm). We chose here two regions where the absorption was minimal and counted fringes at a fixed wavelength while the test cell was being filled to about 250 Torr. The pressure was then determined by counting the number of fringes ΔN between two wavelengths λ_1 and λ_2 at which the refractivities n_1 and n_2 were known and by using a differential form of Eq. (3),

$$P = \frac{760}{273.15}\,\frac{T}{l}\,\Delta N\left(\frac{(n_1-1)}{\lambda_1} - \frac{(n_2-1)}{\lambda_2}\right)^{-1}. \qquad (3a)$$

As a test of the overall method, several measurements were made by counting fringes at a fixed wavelength while filling to $P \gtrsim 760$ Torr and also while evacuating the chamber; the wavelength scan being omitted. These measurements required no quartz-fringe correction and, because they required less time than the usual method, the drift corrections were small. The results of these test measurements are discussed in Sec. III.

D. Experimental uncertainties

High-purity gases and accurate measurements of all parameters in Eq. (3) were required to minimize the uncertainty in the resulting refractivities. In the following paragraphs, we discuss the effects of impurities and the measurements of P, T, l, λ, and N. We present what we estimate to be 90% confidence limits for all uncertainties.

1. Gas purity

The gases used were donated by Airco, Inc.[35] and were of the highest purity commercially available. Each cylinder was analyzed by Airco for trace impurities. The results of these analyses are given in Table I.

The leak and outgas rate of our gas cell was less than 2×10^{-3} Torr/min when the cell was evacuated (and probably much less than this value at the pressures used for the measurements). An assumption that the gas was contaminated at this rate during an entire measurement, which typically took less than 2 h, leads to the conclusion that the partial pressure of impurities was less than 0.3 Torr. This amount of impurities, which would most likely be air, water, or one of the gases studied which had been absorbed onto the walls of the system, would not influence our results by an amount comparable with the uncertainties given in Sec. II D 7.

Evidence that the gas had, in fact, not been contaminated during the measurements is discussed in our earlier paper.[17] One sample of krypton was analyzed after it had been used for refractivity measurements. The analysis, summarized in column 7 of Table I, shows that there were no detectable impurities.

2. Pressure

Our refractivity measurements were usually made by filling the absorption cell to about 5 Torr above the ambient pressure. The difference from the ambient pressure was measured with a Baratron capacitance manometer which had been calibrated by the manufacturer[36] prior to use. The manufacturer's stated possible error for this device was ±0.1% or about ±0.005 Torr. This is much less than the short-term fluctuations of ±0.03 Torr observed in the ambient pressure of the laboratory. The ambient pressure was measured with a mercury barometer.[37] Our barometer was calibrated by comparing it with three other barometers. A description of the instruments and the results of the comparisons are given in Table II. The difference of about 0.5 Torr between the micrometer standard barometer and the digital altimeter is not understood. We chose to use our barometer readings without correction and estimate that the 90% confidence limit of uncertainty is ±0.4 Torr or 0.053%.

TABLE I. Impurities (in ppm) of the gases used in these measurements.

Impurities	H_2 (grade 6)	He (grade 6)	O_2 (grade 4.7)	CO (grade 4)	Kr (grade 4.5)	Kr (grade 4.5 after use [a])
Hydrogen	(bal.) [b]	0.002	···	<5	···	<10
Helium	<2.0	(bal.) [b]	···	···	<1.0	<10
Oxygen	<0.5	0.008	(bal.) [b]	<18	1.0	<10
Carbon monoxide	<1.0	···	···	(bal.) [b]	···	···
Krypton	···	···	9.0	···	(bal.) [b]	(bal.) [b]
Neon	···	0.013	···	···	···	···
Argon	···	0.002	0.7	<18	···	···
Xenon	···	···	···	···	<20.0	<10
Nitrogen	<1.0	0.013	8.8	47	<15.0	<50
Carbon dioxide	<1.0	0.006	···	<10	<1.0	···
Water	···	0.6	···	<2	···	···
Total hydrocarbons	<1.0	···	···	<2	<0.5	<10
Detection methods [c]	MS	MS, MM	MS	GC	MS, OA, HA, ID	MSG

[a] Kr sample analyzed after use in a refractivity measurement. Results of an analysis for impurities performed by Gollub Analytical Services Corp., Berkeley Heights, N. J. 07922.
[b] Balance is main component.
[c] MS: mass spectrometer (detection limit for other impurities 2 ppm); MM: moisture monitor; GC: gas chromatograph; HA: trace hydrogen analyzer; OA: trace oxygen analyzer; ID: infrared nondispersive flame ionization detector; MSG: mass spectrometer (detection limit for other impurities 10 ppm).

3. *Temperature*

The absorption cell was surrounded with a water jacket through which water at a thermostatically controlled temperature flowed at all times. The water also flowed through coils attached to the gas-handling manifold. Because the water temperature was maintained within 1 K of the ambient temperature, and because the surface area of windows and valves, which were not in contact with the water, was small, we assumed that the gas under study was at the temperature of the water bath.

TABLE II. Comparison of readings on different barometers.

Instrument	$P - P_{\text{our barometer}}$
Mercury barometer No. 702 [a] (calibration of February 1973, traceable to U.S. Nat. Bur. Stand.); USNWS [b]	+0.01 Torr
Micrometer standard barometer No. 1948 Hass Instrument Corp. Type MS-2; AFCRL [c]	−0.33 Torr
Sperry digital altimeter-setting indicator, model 4016102-901; AFCRL [c]	+0.18 Torr

[a] This barometer was similar to the one we used.
[b] U.S. Nat. Weather Service, Logan Airport, Boston, Mass.
[c] Air Force Cambridge Research Lab., Bedford, Mass.

The water temperature was measured with thermistors[38] at the input and output to the water jacket. The thermistors were not placed in the water directly but were potted into a copper plug which was in contact with the water. A high-thermal-conductivity epoxy was used.[39] The copper plug was thermally insulated from the water jacket shell by a low-thermal-conductivity Vespiel SP1 plastic insert.[40]

The manufacturer's specifications for the thermistors states that the absolute tolerance is ±0.13 K over the temperature range used. We confirmed this by comparing three thermistors and two mercury thermometers, accurate to ±0.1 K, over a range of temperature from 292 to 310 K. The input and output voltages to the thermistor bridge networks were measured routinely with a digital voltmeter to ±1 mV, which corresponded to ±0.06 K. Readings made with this instrument were frequently verified with the aid of a precision voltmeter accurate to ±0.1 mV. Thus the overall uncertainty in the temperature measurements was limited by the manufacturer's tolerance. Because of the possible additional effect of the surfaces that were not in contact with the water bath, the uncertainty in the temperature of the gas was estimated to be ±0.2 K or ±0.067%.

4. *Length*

The length of the absorption cell was measured with inside micrometers to be (117.18 ± 0.01) cm.

The optical axis was parallel to the axis of the test cell to within 10 mrad. Thus the total uncertainty in the optical path length in the test gas was less than ±0.01%.

5. *Wavelength*

Fringe counts were made at the wavelengths of SiI, SiII, NI, or H_2 lines. The identifications of the lines used are given in Tables IV–VIII. The lines were seen in emission superimposed on the molecular-hydrogen continuum of our light source[41] as shown in the inset to Fig. 1. The wavelengths of the Si and N lines were taken from Moore[42] and from Kelly and Palumbo.[43] Wavelengths from Moore[42] for wavelengths longer than 200 nm were converted to vacuum wavelengths by using the tables of Coleman, Bozman, and Meggers.[44] The wavelengths of the H_2 lines were taken from Schubert and Hudson.[45] These wavelengths were the least accurate of those used but their uncertainty of ±0.01 nm is negligible for our measurements.

The wavelengths of additional strong lines were determined by fitting a three-term polynomial interpolation formula to 47 identified lines between 186 and 163 nm. The identified lines included those listed in Tables IV–VIII as well as 25 lines of molecular hydrogen in the region of $163 < \lambda < 168$ nm. The uncertainty in the fitted wavelengths is estimated to be ±0.02 nm or about ±0.01%.

6. *Fringe counts*

The uncertainty in the fringe counts is primarily that associated with the quartz-fringe and drift corrections. We estimate that this is ±1 fringe for $\lambda > 220$ nm and ±2 fringes for $\lambda < 220$ nm. The percent uncertainty in the fringe count depends on the refractivity of the gas investigated, and thus varies from gas to gas. The uncertainties are listed in Table III.

7. *Resulting uncertainties in refractivities*

The various uncertainties in the results have been assumed to be independent and were combined in the appropriate statistical manner. The total uncertainty (90% confidence limit) is given for each gas and approximate wavelength range in columns 7 and 8 of Table III. We have assumed that only the uncertainties in pressure, temperature, and fringe count had to be considered, as the others were negligible.

For a given gas, the ratio of refractivities at any two wavelengths has a smaller uncertainty than is given in columns 7 and 8 of Table III because the possible errors in the temperature and pressure measurements need not be considered. The uncertainties in such relative refractivities are given essentially by the uncertainties in the fringe counts listed in columns 5 and 6 of Table III.

8. *Checks on uncertainty estimates*

Confirmation that our estimates of expected experimental uncertainties are valid can be obtained by comparing our results with other refractivity data. Unfortunately, there are few other accurate data in our wavelength range. Exceptions are the theoretical data for helium, which will be dis-

TABLE III. Estimated uncertainties in refractivity data (90% confidence limit).

Gas	Special conditions [a]	Fringe number N (approximate) $\lambda < 220$ nm	Fringe number N (approximate) $\lambda > 220$ nm	$\Delta N/N$ (%) $\lambda < 220$ nm	$\Delta N/N$ (%) $\lambda > 220$ nm	Uncertainty in refractivity (%) [b] $\lambda < 220$ nm	Uncertainty in refractivity (%) [b] $\lambda > 220$ nm
He		180	155	1.1	0.64	1.1	0.65
	2 atm [c]	360	310	0.56	0.32	0.58	0.35
H_2		1000	670	0.20	0.15	0.22	0.17
CO			1670		0.060		0.10
		350 [d]		0.57		0.58	
O_2		1750	1350	0.22 [e]	0.074	0.24	0.11
	$\lambda < 197$ nm	400		0.5		1.0 [f]	
Kr		3000	2100	0.067	0.048	0.11	0.10
	$\lambda < 190$ nm, $P = 1$ atm [g]	3000		0.10		0.13	
	$\lambda < 190$ nm, $P = 0.25$ atm [h]	700		0.29		0.3	

[a] Special conditions are explained in detail in Sec. II C.
[b] Total uncertainty calculated with relative uncertainties of ±0.053% for the pressure and ±0.067% for the temperature.
[c] Uncertainty in pressure was ±0.13%.
[d] Pressure was 100 Torr in order to avoid absorption by the fourth positive system of CO.
[e] Uncertainty in fringe count is assumed to be ±4, as only one plate was measured.
[f] Uncertainty limited by pressure determination (see Sec. II C).
[g] Uncertainty in fringe count was ±3.
[h] Uncertainty in fringe count was ±2.

TABLE IV. Refractivity of helium $(n-1)$ $(\times 10^{-6})$.

λ_{vac} (nm)	Identification [a]	This experiment	Theory [b]	Δ(%) [c]	Other measurements	Δ(%) [c]
288.24	Si I 43	35.54	35.54	0.0		
263.21	Si I 83	35.74	35.75	−0.03		
253.7			35.85		35.49 [d]	+1.01
252.93	Si I 1	35.87	35.85	+0.06		
251.69	Si I 1	35.91	35.87	+0.11		
250.77	Si I 1	35.89	35.88	+0.03		
243.59	Si I 45	35.97	35.96	+0.03		
228.8			36.16		36.01 [d]	+0.42
221.74	Si I 3	36.34	36.27	+0.19		
221.16	Si I 3	36.31	36.28	+0.08		
220.87	Si I 3	36.32	36.29	+0.08		
213.9			36.41		36.34 [d]	+0.19
212.48	Si I 48	36.48	36.44	+0.11		
205.88	Si I 52	36.63	36.57	+0.16		
198.90	Si I 7	36.78	36.72	+0.16		
198.32	Si I 7	36.75	36.74	+0.03		
194.2			36.84		36.90 [d]	−0.16
190.13	Si I 57	37.05	36.94	+0.30		
190			36.95		37.7 [e]	−2.0
185.07	Si I 10	37.17	37.09	+0.22		
184.9			37.09		37.18 [d]	−0.24
184.75	Si I 10	37.19	37.09	+0.27		
182.0			37.18		37.20 [d]	−0.05
180			37.25		37.3 [e]	−0.1
177.09	Si I 14	37.45	37.35	+0.27		
174.27	N I 9	37.46	37.45	+0.03		
172.26	Si I 81.04	37.65	37.52	+0.35		
171.34	Si I 81.05	37.66	37.56	+0.27		
170.44	Si I 17	37.70	37.59	+0.29		
170.16	*	37.71	37.60	+0.29		
170.2			37.60		37.65 [f]	−0.13
170			37.61		37.4 [e]	+0.6
169.91	*	37.74	37.61	+0.34		
168.46	*	37.81	37.67	+0.37		
167.96	*	37.82	37.69	+0.34		

[a] Multiplet numbers from Refs. 42 and 43. Asterisks indicate that computed wavelengths were used (cf. Sec. II D 5).

[b] Victor, private communication (Ref. 28).

[c] Percent difference between experimental values and theoretical data.

[d] Abjean, Méhu, and Johannin-Giles (Ref. 14).

[e] Huber and Tondello (Ref. 19).

[f] Bideau-Méhu, Guern, Abjean, and Johannin-Gilles (Ref. 18).

cussed in Sec. III A, and measured as well as interpolated values for standard air.[46] Data for the refractivity of standard air measured with our apparatus[47] differ from those of Eldén[46] by $(0.16 \pm 0.02) \times 10^{-6}$ in 330×10^{-6}; i.e., by 0.048%. The uncertainty of $\pm 0.02 \times 10^{-6}$ represents the standard deviation in the difference calculated at seven wavelengths for three separate measurements. It reflects random errors that are about of the size expected if one assumed that the fringe count could be determined to an accuracy of ±0.1 fringe from our photoelectric chart recordings and to ±0.2 fringe from the photographs. An error in our drift or quartz-fringe corrections would most likely manifest itself as a systematic error with wavelength, but no wavelength dependence of the difference between our work and that of Eldén is discernible.

Thus we conclude that our corrections, and our results, are probably more accurate than is indicated by the uncertainty estimates given in Table III.

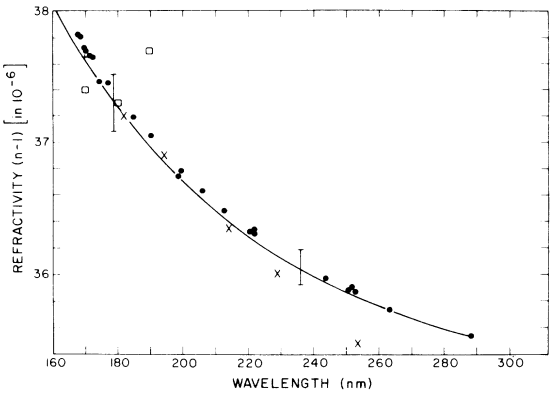

FIG. 3. Refractivity of helium (He) vs wavelength: ●, experimental values from this work; ×, +, and □, previous experiments by, respectively, Abjean *et al.*, Bideau-Méhu *et al.*, and Huber and Tondello (Refs. 14, 18, and 19). The solid line represents the theoretical values of Victor (Ref. 28). Typical uncertainties in our measurements are shown. For simplicity, the data of Leonard (Ref. 1) have been omitted; they would be represented by a line parallel to, but 0.2% above, that shown.

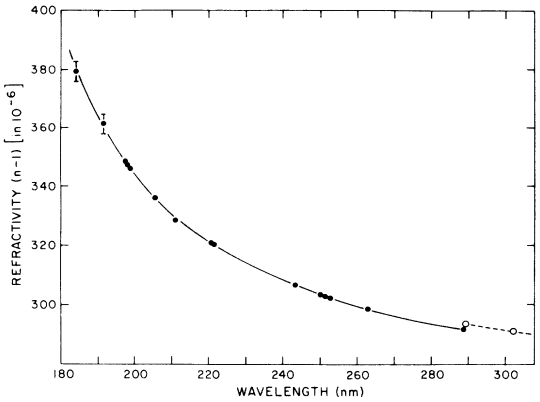

FIG. 5. Refractivity of oxygen (O_2) vs wavelength: ●, experimental values from this work; ○, experimental data from J. T. Howell, Phys. Rev. 6, 81 (1915), listed in Ref. 7. The solid line represents the fit to our data, but this cannot be used to obtain accurate refractivity values in the region of the molecular bands. The dashed line is a fit to the data of Howell. Our experimental uncertainties are shown where they are larger than the symbols.

III. RESULTS AND COMPARISON WITH OTHER DATA

In the following paragraphs, our data will be compared with other measured values and with theoretical calculations. In order to compare with the literature values, which were measured at wavelengths different from those we used, interpolations of our results were required. For H_2 and Kr, we fitted a three-term formula of the Sellmeir type [similar to Eq. (1a)] to our data. We did not attempt to extract any physical significance (i.e., oscillator strengths) from the fit to the data, as we were striving only for the best fit for interpolation and comparison purposes. Consequently, negative terms in the Sellmeir formula were allowed. In the case of CO, three-term Lagrange interpolation was used. Fitting parameters were adjusted until the deviations between the data and the fitted points were less than

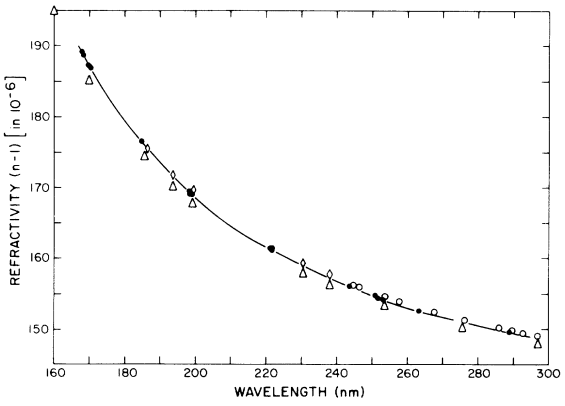

FIG. 4. Refractivity of hydrogen (H_2) vs wavelength: ●, experimental values from this work; △, theoretical data from Ford (Ref. 29); ◇ and ○, previous experiments by Kirn (Ref. 31) and by Koch (Ref. 30), respectively. The solid line represents the fit to our data. Our experimental uncertainties are smaller than the symbols.

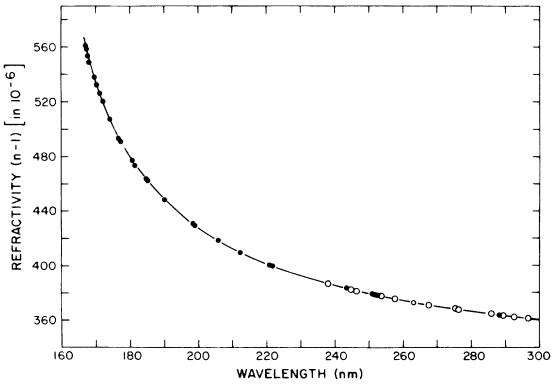

FIG. 6. Refractivity of carbon monoxide (CO) vs wavelength: ●, experimental values from this work; ○, experimental data from J. Koch, Ark. Mat. Astron. Fys. 10, (1914), listed in Ref. 7. The solid line represents a fit to our data but this cannot be used to obtain accurate refractivity values in the region of the bands belonging to the fourth positive system. Our experimental uncertainties are smaller than the symbols.

TABLE V. Refractivity of hydrogen $(n-1)$ $(\times 10^{-6})$.

λ_{vac} (nm) [a]	This expt.	Interpolated value [b]	Δ(%) [c]	Theory [d]	Δ(%) [e]	Previous expt. [f]	Δ(%) [e]	Previous expt. [g]	Δ(%) [e]
289.45		149.3		148.5	+0.5	149.9	−0.4	149.9	−0.4
288.24	149.7	149.4	+0.2	148.6	+0.5				
275.36		150.9		150.2	+0.5	151.5	−0.4	151.5	−0.4
263.21	152.8	152.7	+0.1	151.7	+0.7				
253.56		154.2		153.2	+0.7	154.7	−0.3	154.7	−0.3
252.93	154.4	154.3	+0.1	153.3	+0.7				
251.69	154.6	154.6	0.0	153.5	+0.7				
250.77	154.8	154.7	+0.1	153.7	+0.7				
243.59	156.1	156.1	0.0	155.0	+0.7				
237.91		157.3		156.2	+0.7	157.7	−0.3	157.7	−0.3
230.29		159.1		157.8	+0.8	159.4	−0.2	159.4	−0.2
221.74	161.4	161.4	0.0	160.0	+0.9				
221.16	161.5	161.5	0.0	160.2	+0.8				
220.89	161.6	161.6	0.0	160.3	+0.8				
212.48	164.1	164.3	−0.1	162.8	+0.9				
205.88	166.5	166.6	−0.1	165.0	+1.0				
199.05		169.4		167.7	+1.0	170.6 [h]	−0.7	169.4	0.0
198.90	169.3	169.5	−0.1	167.8	+1.0				
198.32	169.6	169.7	−0.1	168.0	+1.0				
197.76	169.8	170.0	−0.1	168.2	+1.1				
193.58		171.9		170.1	+1.0	172.1 [h]	−0.1	171.8	+0.1
190.13	173.7	173.7	0.0	171.8	+1.1				
186.27		175.8		173.9	+1.1	176.0 [h]	−0.1	175.5	+0.2
185.46		176.3		174.4	+1.1	176.4 [h]	−0.1	176.0	+0.2
185.07	176.4	176.5	−0.1	174.6	+1.1				
184.75	176.6	176.7	−0.1	174.8	+1.1				
181.69	178.5	178.6	−0.1	176.6	+1.1				
177.09	181.7	181.7	0.0	179.6	+1.2				
172.23	185.4	185.4	0.0	183.2	+1.2				
171.34	186.1	186.2	−0.1	183.9	+1.2				
170.45	186.9	186.9	0.0	184.7	+1.2				
169.91	187.6	187.4	+0.1	185.2	+1.2				
169.79	187.8	187.5	+0.2	185.3	+1.2				
168.46	188.7	188.7	0.0	186.4	+1.2				
167.97	189.2	189.1	+0.1	186.9	+1.2				

[a] Line identifications are given in Table IV, except for the lines at 181.69 nm (Si II, uv mult. 1) and at 169.79 nm (Si I, uv mult. 18) (Ref. 43).
[b] Interpolation by a two-term Sellmeir formula.
[c] Percent difference between our experimental data and the fit to our data.
[d] Theoretical values from Ford (Ref. 29).
[e] Percent difference between fit to our data and literature value.
[f] Previous experiment: Koch (Ref. 30).
[g] Previous experiment: Kirn (Ref. 31).
[h] Extrapolated values.

the expected relative uncertainty in the data.

In the case of He, our data and those of other experimenters could be compared directly with theoretical values; thus no interpolation was required. For O_2, most of the previously measured data were for wavelengths longer than those studied in this experiment. Linear interpolation and extrapolation were used to compare our results with these data.

A. Helium

Our results and other experimental and theoretical data are given in Table IV and Fig. 3. The experimental data of Abjean *et al.*[14] and of Huber and Tondello[19] have an uncertainty of ±2%. The theoretical values of Victor[28] and of Victor *et al.*[27] have an uncertainty of ±0.1%.[28] The refractivity data given by Leonard[1] are 0.2% larger than the

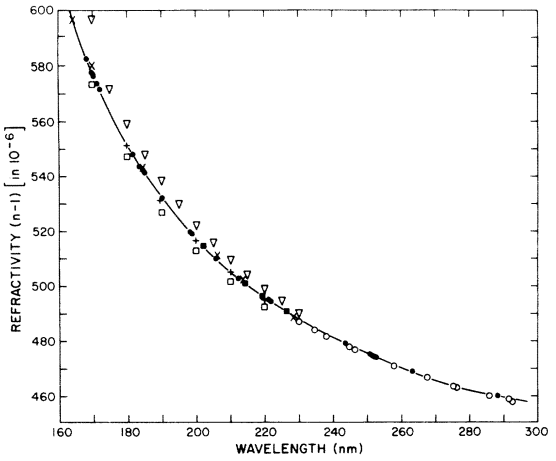

FIG. 7. Refractivity of krypton (Kr) vs wavelength: ●, this work; X, Bideau-Méhu *et al.* (Ref. 18); ○, J. Koch, K. Fysiog. Saellsk. Lund. Förh. 19, 173 (1949), as listed by Leonard (Ref. 1); ▽, Chaschina and Shreider (Ref. 20); ■, W. Kronjäger, Z. Phys. 98, 17 (1936), and dissertation, Technische Hochschule Braunschweig (1934), as listed by Leonard (Ref. 1); +, refractivities derived from absorption measurements by A. E. Kingston, J. Opt. Soc. Am. 54, 1145 (1964); □, semiempirical data by P. W. Langhoff and M. Karplus, J. Opt. Soc. Am. 59, 863 (1967). The solid line represents the fit to our data. Our experimental uncertainties are smaller than the symbols.

TABLE VI. Refractivity of oxygen $(n-1)$ $(\times 10^{-6})$.

λ_{vac} (nm) [a]	Expt.
288.24	291.6
263.21	298.6
252.93	302.4
252.49	302.7
252.00	302.7
251.69	302.9
251.51	303.0
250.77	303.3
243.59	306.5
221.74	320.1
221.16	320.6
220.87	320.8
212.48	328.5
205.88	336.1
198.90	346.2
198.64	346.7
198.32	347.1
198.06	347.6
197.92	347.9
197.76	348.2
191.85 [b]	361.2
184.30 [b]	379.2

[a] Line identifications are given in Table IV, except for the lines at 252.49, 252.00, and 251.51 nm (Si I, uv mult. 1) and at 198.64, 198.06, 197.92, and 197.76 nm (Si I, uv mult. 7) (Ref. 43).

[b] These wavelengths, accurate to ±0.1 nm, do not correspond to spectral lines.

theoretical values throughout the wavelength range 230–500 nm. For simplicity, the results compiled by Leonard were omitted from Table IV and Fig. 3.

Our data are the average of, typically, two measurements at each wavelength, the mean absolute deviation between the measurements being 0.27%.

TABLE VII. Refractivity of carbon monoxide $(n-1)$ $(\times 10^{-6})$.

λ_{vac} (nm) [a]	This expt.	Prev. expt. [b]	Δ(%) [c]
289.4	363.2 [d]	363.3	−0.03
288.24	363.5		
285.8	364.2 [d]	364.4	−0.05
276.1	367.6 [d]	367.7	−0.03
275.4	367.8 [d]	368.0	−0.05
267.6	371.0 [d]	371.0	0.00
263.21	372.9		
257.7	375.5 [d]	375.4	+0.03
253.6	377.6 [d]	377.4	+0.05
252.93	377.9		
251.69	378.4		
250.77	379.1		
246.5	381.5 [d]	381.3	+0.05
244.8	382.5 [d]	382.3	+0.05
243.59	383.2		
237.9	387.0 [d]	386.7	+0.08
221.74	400.1		
221.16	400.5		
220.87	400.8		
212.48	409.9		
205.88	418.6		
198.90	429.9		
198.32	430.9		
190.13	448.6		
185.07	462.8		
184.75	463.7		
181.69	473.8		
180.80	477.3		
177.09	492.9		
174.27	507.6		
172.26	520.2		
171.34	526.6		
170.44	532.3		
169.91	536.5		
168.46	549.1		
167.96	553.8		
167.44	558.6		
167.20	561.2		

[a] Line identifications are given in Table IV, except for the lines at 181.69 and 180.80 nm (Si II, uv mult. 1, Ref. 43), at 167.44 nm (H_2, Ref. 45), and at 167.20 nm. The wavelength of the last line was interpolated (see Sec. II D 5).

[b] Previous experiment: J. Koch, Ark. Mat. Astron. Fys. 10, (1914), as listed in Ref. 7.

[c] Percent difference between fit to our data and literature values.

[d] Refractivity computed from three-term Lagrange fit to our data.

TABLE VIII. Refractivity of krypton $(n-1)$ $(\times 10^{-6})$.

λ_{vac} (nm) [a]	This experiment	Interpolated value [b]	Δ(%) [c]	Previous experiment [d]	Δ(%) [e]	Previous experiments [f]	Δ(%) [e]
298.06		457.2				457.39	−0.04
292.54		458.8				459.24	−0.10
289.36		459.7				460.17	−0.10
288.24	460.1	460.1	0.00				
285.70		460.9				461.38	−0.10
283.69		461.5				461.81	−0.07
275.97		464.2				464.71	−0.11
275.38		464.4				464.99	−0.13
274.86		464.6				464.89	−0.06
267.50		467.5				468.04	−0.12
263.21	469.2	469.3	−0.02				
257.63		471.8				472.36	−0.12
257.31		471.9				472.21	−0.07
252.93	474.1	474.1	0.00				
251.69	474.7	474.7	0.00				
250.77	475.3	475.2	+0.02				
246.41		477.5				478.15	−0.14
244.69		478.5				479.10	−0.13
243.59	479.1	479.1	0.00				
238.00		482.5				483.18	−0.14
234.56		484.8				485.42	−0.13
232.93		485.9				486.17	−0.06
230.21		487.9				488.45	−0.11
228.8		489.0		489.0	0.00		
226.50		490.7				490.89	−0.04
221.74	494.5	494.5	0.00				
221.16	495.0	495.0	0.00				
220.87	495.3	495.3	0.00				
219.46		496.5				496.64	−0.03
214.44		501.2				501.26	−0.01
213.9		501.8		502.3	−0.10		
212.48	503.2	503.2	0.00				
206.2		510.0		510.8	−0.16		
205.88	510.4	510.4	0.00				
202.55		514.4				514.93	−0.10
198.90	519.2	519.2	0.00				
198.32	520.0	520.0	0.00				
197.76	520.7	520.8	−0.02				
190.13	532.6	532.5	+0.02				
185.07	541.7	541.7	0.00				
184.75	542.3	542.3	0.00				
184.4		543.0		543.3	−0.06		
183.65	544.4	544.4	0.00				
181.69	548.4	548.5	−0.02				
180.80	550.4	550.4	0.00				
177.09	559.0	558.9	+0.02				
174.27	565.8	566.1	−0.05				
172.26	571.6	571.5	+0.02				
171.34	574.1	574.1	0.00				
170.44	576.6	576.7	−0.02				
170.2		577.4		580.1	−0.46		
169.91	578.4	578.3	+0.02				
168.46	582.8	582.8	0.00				
167.96	584.3	584.4	−0.02				
164.1		597.7		597.3	+0.07		

[a] Line identifications are given in Table VI, except for the lines at 197.76 nm (Si I, uv mult. 7), 183.65 nm (Si I, uv mult. 11), and at 181.69 and 180.80 nm (Si II, uv mult. 1) (Ref. 43).

[b] Interpolation by a two-term Sellmeir formula.

[c] Percent difference between our experimental data and the interpolated value.

[d] Previous experiment: Bideau-Méhu, Guern, Abjean, and Johannin-Gilles (Ref. 18).

[e] Percent difference between fit to our data and literature value.

[f] Previous experiments: W. Kronjäger, Z. Phys. 98, 17 (1936); dissertation, Technische Hochschule Braunschweig, (1934) (unpublished); J. Koch, K. Fysiogr. Saellsk. Lund. Förh. 19, 173 (1949) cited by Leonard (Ref. 1).

Our data show a systematic deviation from the theoretical calculations which increases to 0.35% at the shorter wavelengths. These deviations are, however, consistent with our expected uncertainties, which range from about ±0.6% at short wavelengths to ±0.35% at longer wavelengths (cf. Table III).

Data at 174.27 and 185.07 nm, obtained by counting fringes while filling and evacuating at a fixed wavelength, showed a smaller deviation from the theoretical results than did the measurements made in the normal manner (cf. Sec. II C).

B. Hydrogen

Our data for the refractivity of H_2, the theoretical data of Ford,[29] which are based upon those of Ford and Browne,[48] and the experimental data of Koch[30] and Kirn[31] are given in Table V and Fig. 4. The theoretical data are calculated for a population distribution corresponding to 300 K. Our values show a systematic deviation from those of Ford and Browne,[48] being 0.7% larger at 288 nm and 1.3% larger at 170 nm. These deviations are four to six times larger than our estimated possible experimental error, which is about 0.2% (cf. Table III). Ford[29] has given a tentative explanation for the discrepancy. Information obtained from Airco, Inc.[35] indicated that the gas would be in the *ortho-para* ratio of 3 : 1 and thus an explanation of the discrepancy, based upon an *ortho-para* ratio other than the normal one, can be excluded.

Our results are about 0.2% smaller than those of Koch[30] and Kirn[31]; this discrepancy is in accord with the mutual error limits. Our data extend the wavelength range for which experimental values are available to 168 nm, i.e., below the lower limit of the work of Kirn[31] at 185 nm.

C. Oxygen

The results for O_2 are given in Table VI and Fig. 5. To the best of our knowledge, there are no other refractivity values below 275.3 nm. A linear extrapolation of our data from 288.2 to 289.4 nm showed that the datum for 289.4 nm given in Ref. 7 is about 0.8% larger than that indicated by our measurement. This discrepancy is larger than the uncertainty of ±0.1% in our results (cf. Table III). The refractivity value given in Ref. 7 for 275.3 nm is about 10% higher than our value, and consequently was omitted from Fig. 5.

D. Carbon monoxide

The refractivities for CO are given in Table VII and Fig. 6. The literature values[7] are limited to wavelengths longer than 230 nm and agree with our results to within our experimental uncertainty of ±0.1% (cf. Table III). Our data extend to 168 nm with uncertainties ranging from ±0.1% to ±0.6% (cf. Table III).

E. Krypton

Our data for Kr, which have an uncertainty of ±0.1% (cf. Table III), are given in Table VIII and Fig. 7. Slight changes from our previously published data[17] have resulted from an improved calculation of the drift correction.

The discrepancy between our data[17] and that of Abjean *et al.*[15] has been investigated by Bideau-Méhu *et al.*[18] Their results confirm our measurements.

ACKNOWLEDGMENTS

This work was supported in part by NASA Grant No. NGL-22-007-006. We also gratefully acknowledge the support of Airco, Inc., Rare and Specialty Gases Division, and the technical assistance of Wm. E. Millikin, and W. Menzi. We thank R. Dorr of the U. S. National Weather Service at Logan Airport, Boston, S. Münch of the Air Force Cambridge Research Laboratory, Bedford, Massachusetts and L. G. Rubin of Francis Bitter National Magnet Laboratory at the Massachusetts Institute of Technology for giving us access to accurate and calibrated barometers and thermometers, and for their generous help. We also wish to thank A. L. Ford, H. P. Palenius, and G. A. Victor for useful discussions and for permitting us to use their results in advance of publication.

---

*A preliminary report of this work was given at the Atomic Spectroscopy Symposium, National Bureau of Standards, Sept. 23–26, 1975.

[1]P. J. Leonard, At. Data Nucl. Data Tables 14, 21 (1974).

[2]J. O. Hirschfelder, C. F. Curtis, and R. B. Bird, *Molecular Theory of Gases and Liquids* (Wiley, New York, 1954), pp. 877–898.

[3]G. A. Victor and A. Dalgarno, J. Chem. Phys. 50, 2535 (1969).

[4]M. J. S. Belton, M. B. McElroy, and M. J. Price, Astrophys. J. 164, 191 (1971).

[5]L. Wallace, Astrophys. J. 176, 249 (1972).

[6]S. P. Tarafdar and M. S. Vardya, Mon. Not. R. Astron. Soc. 162, 299 (1973).

[7]*International Critical Tables*, edited by E. W. Washburn (McGraw-Hill, New York, 1930), Vol. VII, pp. 2–11.
[8]E. R. Peck and D. J. Fisher, J. Opt. Soc. Am. 54, 1362 (1964).
[9]E. R. Peck and B. N. Khanna, J. Opt. Soc. Am. 56, 1059 (1966).
[10]C. R. Mansfield and E. R. Peck, J. Opt. Soc. Am. 59, 199 (1969).
[11]E. R. Peck and K. Reeder, J. Opt. Soc. Am. 62, 958 (1972).
[12]A. Pery-Thorne, J. Quant. Spectrosc. Radiat. Transfer 2, 427 (1962).
[13]R. Abjean, A. Méhu, and A. Johannin-Gilles, C. R. Acad. Sci. B 271, 411 (1970).
[14]R. Abjean, A. Méhu, and A. Johannin-Gilles, C. R. Acad. Sci. B 271, 835 (1970).
[15]R. Abjean, A. Méhu, and A. Johannin-Gilles, Opt. Commun. 3, 45 (1971).
[16]A. Bideau-Méhu, Y. Guern, R. Abjean, and A. Johannin-Gilles, Opt. Commun. 9, 432 (1973).
[17]P. L. Smith, W. H. Parkinson, and M. C. E. Huber, Opt. Commun. 14, 374 (1975).
[18]A. Bideau-Méhu, Y. Guern, R. Abjean, and A. Johannin-Gilles (unpublished).
[19]M. C. E. Huber and G. Tondello, J. Opt. Soc. Am. 64, 390 (1974).
[20]G. I. Chaschina and E. Ya. Shreider, Opt. Spektrosk. 27, 161 (1969) [Opt. Spectrosc. 27, 79 (1969)].
[21]G. I. Chaschina, V. I. Gladushchak and E. Ya. Shreider, Opt. Spektrosk. 24, 1008 (1968) [Opt. Spectrosc. 24, 542 (1968)].
[22]P. G. Wilkinson, J. Opt. Soc. Am. 50, 1002 (1960).
[23]D. W. O. Heddle, R. E. Jennings, and A. S. L. Parsons, J. Opt. Soc. Am. 53, 840 (1963).
[24]P. Gill and D. W. O. Heddle, J. Opt. Soc. Am. 53, 847 (1963).
[25]P. D. Chopra and D. W. O. Heddle, J. Phys. B 7, 2421 (1974).
[26]A. N. Zaidel' and E. Ya. Shreider, *Vacuum Ultraviolet Spectroscopy* (Humphrey, Ann Arbor, 1970), pp. 318–324.
[27]G. A. Victor, A. Dalgarno, and A. J. Taylor, J. Phys. B 1, 13 (1968).
[28]G. A. Victor, private communication.
[29]A. L. Ford, private communication.
[30]J. Koch, Ark. Mat. Astron. Fys. 8 (No. 20), 1 (1913).
[31]M. Kirn, Ann. Phys. (Leipz.) 64, 566 (1921).
[32]F. P. Banfield, M. C. E. Huber, W. H. Parkinson, and E. F. Tubbs, Appl. Opt. 12, 1279 (1973).
[33]J. Hilsenrath, *Tables of Thermal Properties of Gases*, Circ. U. S. Nat. Bur. Stand. No. 564 (U. S. GPO, Washington, D. C., 1955).
[34]J. M. H. Sengers, M. Klein, and J. S. Gallagher, in *American Institute of Physics Handbook*, edited by D. E. Gray (McGraw-Hill, New York, 1972), third ed., Chap. 4i, pp. 4-204–4-221.
[35]Airco, Inc., Rare and Specialty Gases Division, Murray Hill, N. J. 07974.
[36]MKS Instruments, Burlington, Mass. 01803.
[37]U. S. Army Signal Corps type, CENCO 76894 (Central Scientific Co., Chicago, Ill. 60623).
[38]YSI Part No. 44202 (Yellow Springs Instrument Co., Yellow Springs, Ohio 45387).
[39]Delta Bond 152, Hardener A4 (Wakefield Engineering, Wakefield, Mass. 01880).
[40]E. I. DuPont de Nemours & Company, Inc., Wilmington, Del. 19898.
[41]F. J. P. Clarke and W. R. S. Garton, J. Sci. Instrum. 36, 403 (1959).
[42]C. E. Moore, Nat. Stand. Ref. Data. Ser., U. S. Bur. Stand. 3, Sec. 1 (1965) and Sec. 2 (1967).
[43]R. L. Kelly and L. J. Palumbo, *Atomic and Ionic Emission Lines below 2000 Å, Hydrogen through Krypton*, NRL Report 7599 (U. S. Naval Research Laboratory, Washington, 1973).
[44]C. D. Coleman, W. R. Bozman, and W. F. Meggers, *Table of Wavenumbers* (U. S. Nat. Bur. Stand., Washington, D. C. 1960), Monograph 3.
[45]K. E. Schubert and R. D. Hudson, Report No. ATN-64 (9233)-2, Aerospace Corp., Los Angeles, 1963 (unpublished).
[46]B. Edlén, Metrologia 2, 71 (1966).
[47]H. P. Palenius and P. L. Smith (unpublished).
[48]A. L. Ford and J. C. Browne, Phys. Rev. A 7, 418 (1973).

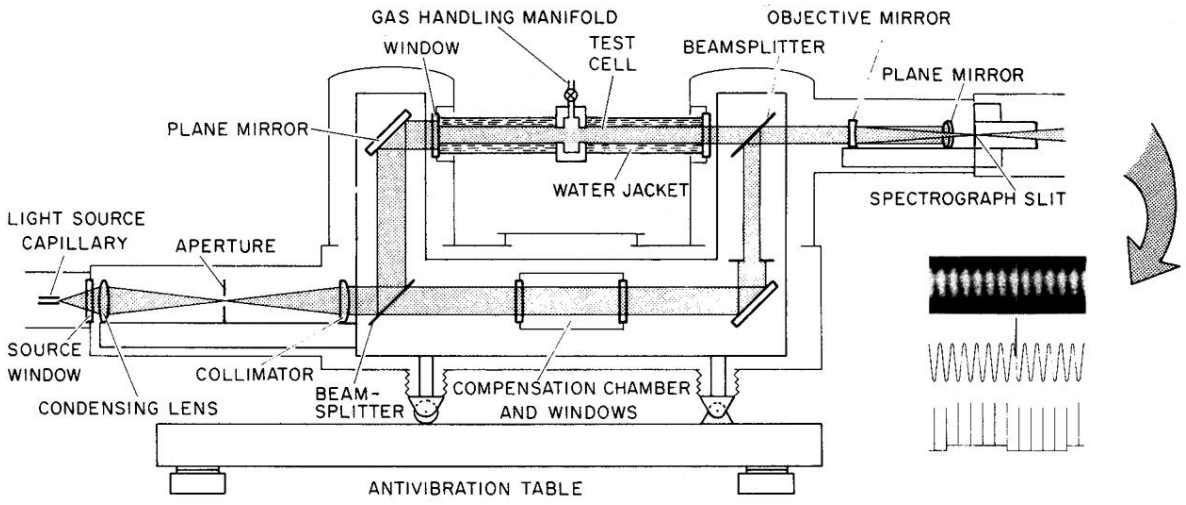

FIG. 1. Schematic of apparatus for refractivity measurements. During a measurement, the spectral display of fringes in the focal plane of the spectrograph can be recorded photoelectrically as well as by photograph, as indicated in the inset. The inset also shows an emission line superimposed on the fringe pattern.